Journal of Nuclear Medicine, published on July 29, 2022 as doi:10.2967/jnumed.122.264361

Static and dynamic ^{68}Ga-FAPI PET/CT for the detection of malignant transformation of intraductal papillary mucinous neoplasia of the pancreas

Running title: FAPI-PET for IPMN

Matthias Lang[1], Anna-Maria Spektor[2], Thomas Hielscher[3], Jorge Hoppner[2], Frederik M. Glatting[2], Felix Bicu[2], Thilo Hackert[1], Ulrike Heger[1], Thomas Pausch[1], Ewgenija Gutjahr[4], Hendrik Rathke[5], Frederik L. Giesel[6], Clemens Kratochwil[2], Christine Tjaden[1], Uwe Haberkorn[2] and Manuel Röhrich[2]

Affiliations:

1 Department of General, Visceral, and Transplantation Surgery, University Hospital Heidelberg, Germany.

2 Department of Nuclear Medicine, University Hospital Heidelberg, Germany.

3 Department of Biostatistics, German Cancer Research Center, Heidelberg, Germany.

4 Department of Pathology, University Hospital Heidelberg, Germany.

5 Department of Nuclear Medicine, The Inselspital, Bern University Hospital, University of Bern, Switzerland.

6 Department of Nuclear Medicine, University Hospital Düsseldorf, Düsseldorf, Germany.

Corresponding Author:

Manuel Röhrich

Im Neuenheimer Feld 400

69120 Heidelberg

Telephone: 0049 6221 56 7731

Fax: 0049 6221 56 5473

Email: manuel.roehrich@med.uni-heidelberg.de

ORCID-ID: 0000-0001-7609-243X

First Author:
Matthias Lang
Im Neuenheimer Feld 420
69120 Heidelberg
Telephone: 0049 6221 56 6110
Fax: 0049 6221 56 6402
Email: matthias.lang@med.uni-heidelberg.de
ORCID-ID: 0000-0003-3585-4287

DECLARATIONS

Funding: This work was funded by the Federal Ministry of Education and Research, grant number 13N 13341.

Conflicts of interest: UH, CK and FLG have filed a patent application for quinoline based FAP targeting agents for imaging and therapy in nuclear medicine. UH, CK and FLG also have shares of a consultancy group for iTheranostics. No other potential conflicts of interest relevant to this article exist.

Ethics approval: All procedures performed in studies involving human participants were in accordance with the ethical standards of the institutional and/or national research committee and with the 1964 Helsinki declaration and its later amendments or comparable ethical standards. This retrospective study was approved by the local institutional review board (study number S-115/2020).

ABSTRACT

Purpose

Pancreatic ductal adenocarcinoma (PDAC) may arise from intraductal papillary-mucinous neoplasms (IPMN) with malignant transformation, but a significant portion of IPMN remains to show benign behavior. Therefore, it is important to differentiate between benign IPMN and IPMN lesions undergoing malignant transformation. However, non-operative differentiation by ultrasound, CT, MRI and carbohydrate antigen 19-9 (CA19-9) is still unsatisfactory. Here, we assessed the clinical feasibility of additional assessment of malignancy by positron emission tomography using ^{68}Gallium-labeled Fibroblast Activation Protein Inhibitors (^{68}Ga-FAPI-PET) in 25 patients with magnetic resonance imaging (MRI) - or computed tomography (CT) - proven cystic pancreatic lesions.

Methods

25 patients with cystic pancreatic lesions who were followed up in the European Pancreas Center of Heidelberg University hospital and who were led to surgical resection or fine needle aspiration (FNA) due to suspicious clinical, laboratory chemistry or radiological findings were examined by static (all patients) and dynamic (20 patients) ^{68}Ga-FAPI-PET. Cystic pancreatic lesions were delineated and maximum and mean standardized uptake values (SUV_{max} / SUV_{mean}) were determined. Time activity curves and dynamic parameters (time to peak, K1, k2, K3, k4) were extracted from dynamic PET data. Receiver operating curves (ROC) of static and dynamic PET parameters were calculated.

Results

11 of the patients suffered from menacing IPMN (high grade IPMN with (6 cases) or without (5 cases) progression into PDAC) and 11 from low grade IPMN, 3 patients from other benign entities. Menacing IMPN showed significantly elevated ^{68}Ga-FAPI uptake compared to low grade IPMN and other benign cystic lesions. In dynamic imaging, menacing IPMN showed increasing time activity curves (TAC) followed by slow decrease afterwards, TAC of low grade IPMN showed an immediate peak followed by rapid decrease for about 10 minutes and slower decrease for the rest of the time. ROC curves

showed high sensitivity and specificity (area under the curve (AUC) greater than 80%) of static and dynamic PET parameters for the differentiation of IPMN subtypes.

Conclusion

^{68}Ga-FAPI-PET is a helpful new tool for the differentiation of menacing and low grade IPMN and shows the potential to avoid unnecessary surgery for non-malignant pancreatic IPMN.

Keywords: Fibroblast Activation Protein, FAPI, PET, dynamic PET, Cancer, PDAC, IPMN

INTRODUCTION

The pancreatic ductal adenocarcinoma (PDAC) belongs to the most lethal cancers with a poor 5-year survival rate of less than 10% despite surgical resection, radiotherapy and chemotherapy (*1*). Intraductal papillary mucinous neoplasms (IPMN) with high grade dysplasia (hg-IPMN) are precursors for malignant transformation into PDAC (*2*). Therefore, resection of hg-IPMN before the development of invasive PDAC is mandatory (*3,4*). Hg-IPMN with and without development into PDAC are grouped together in this article as menacing IPMN (men-IPMN). In contrast, IPMN with low-grade dysplasia (lg-IPMN) are regarded as benign lesions which should be controlled regularly, but not resected (*3,4*). Regarding the significant risk of complications in pancreatic surgery (morbidity rates of 35-50% and mortality rates up to 1% (*5,6*)), the selective resection of men-IPMN is an important goal.

Currently, evaluation of IPMN regarding malignant potential is controversial and mostly based on the Fukuoka consensus criteria of 2017 or the European guidelines for pancreatic cystic neoplasms. Both rely on multiple clinical and morphological parameters (*3,4*). However, several publications have shown the shortcomings of these guidelines due to their limited specificity and sensitivity (*7-9*). Recent studies revealed that only 35 % of IPMN were resected in a timely fashion (*10*). Therefore, the decision for surgical treatment remains challenging and clinical tools to distinguish between lg-IPMN and men-IPMN are urgently needed.

Positron emission tomography using ^{68}Gallium-labelled Fibroblast Activation Protein Inhibitors combined with computed tomography (^{68}Ga-FAPI PET/CT) has shown excellent imaging properties and high clinical potential for PDAC. The intense FAPI-tracer accumulation in PDAC is based on their vast stromal portion including Fibroblast Activation Protein (FAP)-positive cancer-associated fibroblasts (CAFs) (*11*). We hypothesized that FAP-positive stroma could be a common feature of PDAC and men-IPMN, but not of lg-IPMN, as the desmoplastic stromal reaction is a prominent hallmark of malignancy, but not of benign lesions (*12*). Here, we retrospectively analyzed preoperative static and dynamic ^{68}Ga-FAPI-PET data of 25 patients with suspected IPMN

and compare imaging features with histological diagnoses to evaluate the potential value of ^{68}Ga-FAPI-PET for the differentiation of lg- and men-IPMN.

MATERIALS AND METHODS

Patient characteristics

Patients were selected for ^{68}Ga-FAPI-PET according to the following criteria: aged 18 years or older, MRI- or CT-proven pancreatic cyst leading to the clinical diagnosis of IPMN, absolute or relative indication for surgery, sufficient compliance for and consent to the ^{68}Ga-FAPI-PET procedure. All patients conforming to these selection criteria who presented in the European Pancreas Center Heidelberg during the examination period (06/2020 to 12/2021) were included into our analysis. 25 patients (mean age 63.8 yrs, max 83, min 38; 13 male) with contrast enhanced MRI- (24 patients) and/or CT- (2 patients) proven cystic pancreatic lesions planned for surgery were subjected to ^{68}Ga-FAPI-PET imaging. All patients were referred by their treating physicians in order to exclude metastatic disease. Additionally, in 8 patients an EUS guided fine needle aspiration (FNA) cytology was obtained. None of them obtained a malignant result. Clinical diagnosis of IPMN was based on the identification of a cystic lesion >10 mm, related to the pancreatic main duct, or a main duct dilatation of more than 5 mm without signs of chronic pancreatitis in the imaging techniques mentioned above. All patients had a relative or absolute indication for pancreatic surgery according to recent european guidelines (*4*). In 7 patients the diameter of the pancreatic main duct exceeded 10 mm, in one patient >5 mm and one patient presented with jaundice. 4 patients showed an elevated carbohydrate antigen 19-9 (CA 19-9) level, 9 a branch duct dilatation >40 mm and in one patient an enhancing mural nodule <5 mm was detected. One female presented symptomatic with recurrent IPMN related acute pancreatitis. Tumor marker CEA was moderately elevated in one individual (3,4 µg/l, ULN 2,5), who had a highly elevated CA 19-9 (476 U/ml, ULN 37) too. The following absolute or relative criteria for resection according to the guideline mentioned above were not observed: EUS guided malignant cytology/histology, growth rate of branch duct IPMN (BD-IPMN) >5 mm per

year and new onset of diabetes mellitus. Table 1 gives a detailed patientwise overview of clinical characteristics and histological diagnoses.

^{68}Ga-FAPI-PET/CT Imaging

Synthesis and labeling of ^{68}Ga-FAPI-74 was conducted as previously described (*13-15*). For PET imaging, a Siemens Biograph mCT Flow scanner was used, according to previously published protocols (*16*). In short, after a low-dose CT without contrast, 3-dimensional PET scans were acquired (matrix, 200 × 200), reconstructions performed, and emission data corrected for attenuation. For all patients, static PET-scans were acquired 60 minutes after administration of 180 - 329 MBq of ^{68}Ga-labeled FAPI-74. In order to characterize early ^{68}Ga-FAPI-74 uptake kinetics, additional dynamic PET-scans were performed in 20 patients as previously described (*16*).

Image evaluation

For static PET-Scans, SUVmax and SUVmean values of cystic pancreatic lesions and healthy organs were analyzed using a volume of interest (VOI) technique. VOIs were defined by an automatic isocontour with a cutoff at 50% of SUVmax. For dynamic PET Imaging analysis, VOIs of cystic lesions and aortal blood were drawn and applied to the entire dynamic dataset. Time activity curves of ^{68}Ga-FAPI-74 uptake were obtained and time to peak (TTP) values (minutes from the beginning of the dynamic acquisition to the SUVmax of the lesion) were derived from these. Kinetic modeling using a 2-compartment model was performed to generate K1 and k2 values. Dynamic data analysis was done using PMOD software (PMOD Technologies Ltd.).

Statistical analysis

Receiver operating curve (ROC) analysis was used to assess discriminative ability of PET parameters. Area under the ROC curve with corresponding 95% confidence interval using Delong’s method (*17*) was computed using R package pROC (*18*).

RESULTS

Histological results and surgical management of the patients

22/25 patients examined by ^{68}Ga-FAPI-PET/CT have undergone resection or EUS-FNA. 6 of these 22 patients suffered from a histologically confirmed (hc) lg-IPMN. 10 of 22 patients suffered from a hc men-IPMN (6 of them with transition into PDAC). In 3/22 patients, EUS-guided fluid aspiration strongly indicated a mucinous lesion without signs of malignancy, so that we considered these cases as clinical lg-IPMN. 3/22 patient had a histological confirmation of other entities than IPMN (2 serous cystic neoplasia, 1 pancreatic intraepithelial neoplasia). 3/25 patients had no histological confirmation. Due to radiological appearance and clinical course, 2 were considered as clinical lg-IPMN and one as clinical hg-IPMN (figure 1). Out of the 10 patients with hc men-IPMN, 5 have undergone distal pancreatectomy, 3 pancreatoduodenectomy, one complete pancreatectomy and one enucleation. Out of 6 patients with hc lg-IPMN, 2 have undergone pancreaticoduodenectomy, one distal pancreatectomy and one enucleation. 2 patients have undergone EUS-FNA only and are still under surveillance without any complications. As ^{68}Ga-FAPI-74 PET imaging did not reveal any metastatic diseases, it did not influence the surgical management of the patients analyzed.

^{68}Ga-FAPI-74 Biodistribution and uptake of men-IPMN and low grade IPMN

Based on static PET images acquired one hour after injection, normal tissues including the healthy part of the pancreas all showed low SUVmax and SUVmean values resulting in low background signal for the analysis of pathologies (figure 2A). Clinical and hc men-IPMN showed markedly higher ^{68}Ga-FAPI-74 uptake than clinical and hc lg-IPMN and other pathologies (figure 3A, B). Of note, hg-IPMN which had already undergone malignant progression into PDAC showed higher SUVmax and SUVmean values compared to those without (supplemental figure 1). Grouped according to surgical management, ^{68}Ga-FAPI-74 uptake of lesions with an indication for surgery (hc and clinical men-IPMN) was significantly higher than that of lesions without (hc and clinical lg-IPMN and other pathologies) (figure 3C, D).

Dynamic imaging

Dynamic ^{68}Ga-FAPI-74 PET was applied to 20 patients (9 with hc men-IPMN, 4 with hc lg-IPMN, 5 with clinical lg-IPMN and 2 with other pathologies (not evaluated)). Time activity curves (TAC) of hc men-IPMN differed markedly from those of hc and clinical lg-IPMN. Whereas hc men-IPMN showed an increasing TAC for about 6 minutes and slowly decreasing TACs afterwards, hc and clinical lg-IPMN showed an immediate peak followed by rapid decrease for about 10 minutes and slower decrease for the rest of the time (figure 4A-C). The delayed increase and prolonged washout of the tracer in men-IPMN compared to lg-IPMN are also reflected by increased TTP (figure 4D). Kinetic modeling using a 2-tissue compartment model revealed decreased K1 and k2 values (figure 4E, F) as well as decreased K3 and k4 values (supplemental figure 2) of men-IPMN compared to lg-IPMN.

Sensitivity and specificity

Figure 5 shows ROC curves displaying the sensitivity and specificity of SUVmax, SUVmean and TTP for the distinction between hc lg-IPMN and hc men-IPMN (A) and between entities requiring surgery or not (B). For all parameters, the area under the curve (AUC) was greater than 80% suggesting a high discriminatory power of static and dynamic ^{68}Ga-FAPI-PET for both questions, whereat TTP showed slightly higher AUC values than static parameters for both questions (for men-IPMN vs. lg-IPMN: 97.2% versus 86.7% (SUVmax) and 88.3% (SUVmean), for indication for surgery 92.6% versus 91.6% (SUVmax) and 81.8% (SUVmean)). Table 2 provides thresholds and specificities at fixed sensitivities of 90% and 80% including 95% confidence intervals for SUVmax, SUVmean and TTP with respect to the discrimination of hc men-IPMN and hc lg-IPMN and given or not-given indication for surgery.

Case vignette

In figure 6 three representative cases are highlighted. The patient with PDAC based on an IPMN is a 68yr old male, who presented in our department with slight jaundice and brown urine. A weight loss of 6 kg in 3 weeks had occurred. Otherwise the patient was completely asymptomatic. Laboratory results revealed a bilirubine of 8,1 mg/dl (ULN 1,0)

and a CA 19-9 of 341,9 U/ml (ULN 37). In cMR-Imaging a double duct sign and several cystic lesions of the pancreatic head were apparent. There was no visible solid mass in the pancreas. The diagnosis of malignant transformation of a mixed type IPMN was made. To exclude extrapancreatic manifestation, a FAPI-PET/CT was obtained. The pancreatic head showed intense ^{68}Ga-FAPI uptake, indicating pancreatic tumor. As no metastatic lesions were apparent, a Whipple procedure was performed. Histologically an adenocarcinoma of the pancreatic head (35 mm), based on a mixed type IPMN with high grade dysplasia was confirmed (pT2, pN2 (19/26), L1, V1, Pn1, G3, R0, CRM+). For the patient with hg-IPMN without progression into PDAC, a female aged 44 years, randomly determined elevated pancreatic enzymes led to an MR examination. This showed dilation of the main pancreatic duct by 10 mm and brunch duct dilation by 16 mm. There were no symptoms of weight loss, abdominal pain, or pancreatitis. Laboratory results for CA 19-9, bilirubin or inflammation were unremarkable; only lipase was slightly elevated (92 U/l, ULN: 63 U/l). A diagnosis of mixed type IPMN was made. FAPI-PET/CT showed a markedly increased SUV_{max} of 4.9. Via robotic assisted distal pancreatectomy, a mixed type IPMN with high grade dysplasia (pTis, N0) was successfully removed.

The patient with lg-IPMN was a 52 yr old female, who complained about abdominal pain. An abdominal ultrasound revealed a 60 mm sized cystic lesion in the pancreatic head without nodules or suspect perfusion in contrast enhanced Ultrasound. This lesion was confirmed in cMRI and classified as 60 mm side branch IPMN. The laboratory results were unremarkable. The medical history included a type 1 diabetes with an onset at 2 years of age, complicated by neuropathy, retinopathy and terminal nephropathy. In FAPI-PET/CT only a low accumulation was observed. As the size exceeded by far the guideline’s limits, the cystic lesion was removed by laparoscopic robotic enucleation. Histologically a large branch duct IPMN with low grade dysplasia was diagnosed.

DISCUSSION

Summary of the results

In this retrospective analysis of ^{68}Ga-FAPI-74 PET imaging in 25 patients with cystic pancreatic lesions we observed significantly higher ^{68}Ga-FAPI-74 uptake measured as SUVmax and SUVmean in men-IPMN than in lg-IPMN and other benign lesions. In dynamic ^{68}Ga-FAPI-PET imaging, men-IPMN and lg-IPMN showed differential kinetic behavior reflected by differences in TTP, K1 and k2 as well as K3 and k4 values. The high diagnostic accuracy of static and dynamic ^{68}Ga-FAPI-74 PET for the differentiation of men-IPMN and lg-PMN was reflected by high AUC values in all ROC curves analyzed. These results suggest that ^{68}Ga-FAPI-74 PET is a promising new imaging technique for the clinical evaluation of pancreatic cystic lesions.

Static and dynamic ^{68}Ga-FAPI-74 PET imaging

We observed a high ^{68}Ga-FAPI-74 uptake in men-IPMN (with and without PDAC) and significantly lower ^{68}Ga-FAPI uptake in lg-IPMN whereas healthy tissues have negligible background activity, leading to excellent contrast for suspicious lesions, similar to those shown by previous studies on FAPI PET/CT in PDAC and other tumors (*19,20*). Next to static imaging results, we could demonstrate that dynamic imaging delivers additional diagnostic information and may improve the clinical classification of lg-IPMN and men-IPMN due to delayed binding and delayed washout of men-IPMN compared to lg-IPMN. These findings are in line with our previously published data on dynamic ^{68}Ga-FAPI-PET imaging in patients with lung cancer and fibrosing interstitial lung diseases, where we observed delayed washout of tumors compared to fibrotic lesions (*16*). Similarly, we could show in a previous project on ^{68}Ga-FAPI-PET in PDAC that PDAC have a delayed washout compared to pancreatitis (*19*). Although the overall experience with dynamic behavior of FAPI-tracers is limited to few publications to date (*16,21,22*), delayed FAPI-washout appears to be sign of malignancy in this imaging method.

Risk stratification of IPMN

To date, a compound of imaging, clinical, and laboratory criteria has been used to estimate the risk of malignant progression of IPMN. Most data exist on results of imaging techniques. Recent studies, mostly postoperative with a retrospective design, concluded that jaundice, a contrast-enhancing solid component or mural nodule, or a ≥10 mm main duct dilatation have a positive predictive value for malignancy of between 56-89% (*23-25*). A cyst size ≥30 mm without other clinical or radiological risk factors has a low positive predictive value for malignant transformation of an IPMN ranging from 27% to 33% (*26-30*). Several studies regarding mostly surgically resected IPMN reported a wide risk range of 37-91% for high-grade dysplasia or cancer for main duct dilatations of 5-9.9 mm (*31-33*). In patients after surgical resection of BD-IPMN, it was found that mural nodules ≥5 mm on EUS have a sensitivity of 73–85% and specificity of 71–100% for the presence of men-IPMN. Imaging detectability of mural nodes ≥10 mm in CT, MRI, US and EUS were 64%, 68%, 89%, and 97%, respectively. Detectability of mural nodes ≥10 mm is excellent in abdominal and endoscopic ultrasound (*34-36*). In summary, main duct dilatation ≥10 mm and mural nodules on ultrasound examination are the both most reliable factors. It must be considered that mural nodules are a rare condition. Next to morphological imaging, positron emission tomography combined with computed tomography (PET/CT) using ^{18}F-fluorodeoxyglucose (^{18}F-FDG) has been applied in IPMN in order to detect malignancy based on increased glucose metabolism. For this approach, several older meta-analyses had calculated sensitivity and specificity rates of 80 to 95% and 60 to 95%, respectively (*37-40*), but more recent studies could not prove a benefit of ^{18}F-FDG-PET/CT in IPMN (*41,42*). Given the low background activity of FAPI radiotracers compared to ^{18}F-FDG in the pancreas and given the promising preliminary results of our study, one would expect that FAPI-PET may be superior to ^{18}F-FDG for the detection of malignancy in IPMN. Based on our data it appears that ^{68}Ga-FAPI-74 PET signal intensity and uptake kinetics offer high specificity and sensitivity for the detection of subtypes and may complement established predictors of malignancy.

Limitations

Despite promising results, several limitations of our analysis must be considered. The major limitation of our study is the relatively small number of patients with IPMN included, especially with respect to dynamic imaging, which was performed in just 9 subjects. According to this, no definite conclusions should be drawn from our data and further studies with higher numbers of patients including intra-individual comparisons of the diagnostic value for IPMN of ^{68}Ga-FAPI-74 PET and other imaging modalities like CT, MRI and ultrasound are necessary to validate our findings. Another limitation arising from the sparsity of dynamic PET data ist that our dataset does not allow a comparison between the discriminatory power of static alone versus dynamic alone versus combined static and dynamic imaging. Another limitation is that not all patients included have undergone biopsy or surgery for definitive confirmation of their diagnoses. Although we considered the appearance of these lesions in MRI and ultrasound and the clinical course of the patients to gain valid clinical classifications, a rest of uncertainty remains for these cases, especially as our information available only reflects the status of the patients during a limited period of follow up. Another limitation is a certain selection bias that may arise from the fact that all patients included into this analysis were referred by a highly specialized outpatient clinic. So, the dataset may not fully reflect the epidemiology of IPMN subtypes. However, a recently published study on the frequency of IPMN subtypes found a similar distribution of hg-IPMN and lg-IPMN (*10*). Taken together, our findings should be interpreted with caution and need confirmation by larger cohorts, optimally in prospective studies.

CONCLUSION

Static and dynamic ^{68}Ga-FAPI-74 PET/CT showed very promising imaging properties for IPMN and predicted the grade of dysplasia of IPMN with high accuracy. We recommend further clinical evaluation of ^{68}Ga-FAPI-74 PET in combination with and comparison to MRT or EUS for the detection of malignant IPMN of the pancreas.

KEY POINTS

Question: Is static and dynamic ^{68}Ga-FAPI-PET helpful for the discrimination of menacing (high grade with and without progression into PDAC) and low grade intraductal papillary mucinous neoplasm of the pancreas?

Pertinent Findings: Menacing IPMN with and without transformation into pancreatic ductal adenocarcinomas (PDAC) showed significantly higher ^{68}Ga-FAPI uptake than low grade IPMN. Dynamic PET parameters (time to peak, K1, k2, K3, k4) differed markedly between menacing and low grade IPMN.

Implications for Patient Care: ^{68}Ga-FAPI-PET showed promising results with respect to the differentiation of menacing and low grade IPMN and should be further evaluated in patients suffering from IPMN or PDAC.

Table 1: Clinical characteristics and histological diagnoses of 25 patients with suspected IPMN and ^{68}Ga-FAPI-74 PET/CT.

Pat. Number	Sex	Age	Cyst size (mm)	IPMN type	Additional information	Surgery/ histology	Histological diagnosis
1	m	52	29	BD		Whipple	lg-IPMN
2	f	52	57	BD		Excision	lg-IPMN
3	m	76	40	BD		Cytology	lg-IPMN
4	f	42	30	BD		Whipple	lg-IPMN
5	m	71	60	BD		Whipple	lg-IPMN
6	f	67	44	BD		Distal pancreatectomy	lg-IPMN
7	m	56	18*	MD	Mural nodule	Enucleation	hg-IPMN
8	m	79	10*	MD		Whipple	hg-IPMN
9	m	53	20*	MD		Distal pancreatectomy	PDAC
10	f	64	11*	MD		Whipple	PDAC
11	m	68	32	BD	MD with dliatation to 4.8 mm, jaundice	Whipple	PDAC
12	f	44	10*	mixed type		Distal pancreatectomy	hg-IPMN
13	f	57	50*	MD		Pancreatectomy	PDAC
14	m	78	90	mixed type	Solide components	Therapy refused	None
15	f	74	25	BD	Size progressing	Distal pancreatectomy	hg-IPMN
16	f	80	42	BD		Distal pancreatectomy	PDAC
17	f	83	45	BD		Distal pancreatectomy	PDAC
18	m	63	30	BD		Cytology (non-conclusive)	None
19	m	77	60	BD		Cytology	None
20	f	64	30	BD		Cytology (non-conclusive)	None
21	f	57	23	BD	Size progressing	None	None
22	m	74	10	BD		None	None
23	f	54	38			Cytology	SCN
24	f	38	38			Distal pancreatectomy	SCN
25	m	62	21			Distal pancreatectomy	PanIN

Abbreviations: f = female, m = male, mm = millimeter, BD = branch duct, MD = main duct, SCN = serous cystic neoplasia, PanIN = Pancreatic intraepithelial neoplasia, *main duct diameter

Table 2: Threshold and specificity at fixed sensitivities of 90% and 80% including 95% confidence intervals for the differentiation between histologically confirmed low grade IPMN versus histologically confirmed menacing IPMN and given versus not given indication for surgery

Endpoint	Parameter	Threshold	Sensitivity (%)		Specificity (%)		TN	TP	FN	FP
lg/men	SUVmax	3.62	90.0	95%CI (55.5-99.7)	66.7	95%CI(22.3-95.7)	4	9	1	2
		4.85	80.0	95%CI (44.4-97.5)	83.3	95%CI(35.9-99.6)	5	8	2	1
lg/men	SUVmean	2.07	90.0	95%CI(55.5-99.7)	83.3	95%CI(35.9-99.6)	5	9	1	1
		2.19	80.0	95%CI(44.4-97.5	83.3	95%CI(35.9-99.6)	5	8	2	1
lg/men	TTP	135.00	88.9	95%CI(51.8-99.7)	100.0	95%CI(39.8-100.0)	4	8	1	0
		225.00	77.8	95%CI(40.0-97.2)	100.0	95%CI(39.8-100.0)	4	7	2	0
Surgery	SUVmax	3.62	90.9	95%CI(58.7-99.8)	71.4	95%CI(41.9-91.6)	10	10	1	4
		4.85	81.8	95%CI(48.2-97.7)	92.9	95%CI(66.1-99.8)	13	9	2	1
Surgery	SUVmean	2.07	90.9	95%CI(58.7-99.8)	64.3	95%CI(35.1-87.2	9	10	1	5
		2.19	81.8	95%CI(48.2-97.7)	71.4	95%CI(41.9-91.6)	10	9	2	4
Surgery	TTP	135	88.9	95%CI(51.8-99.7)	83.3	95%CI(51.6-97.9)	10	8	1	2
		225	77.8	95%CI(40.0-97.2)	91.7	95%CI(61.5-99.8)	11	7	2	1

lg/men: histologically confirmed low grade IPMN versus histologically confirmed menacing IPMN, TTP = time to peak, CI = confidence interval, TN = true negative, TP = true positive, FN = false negative, FP = false positive. For some settings only approximate sensitivities could be selected due to sparsity of data.

Figures and figure captions

Figure 1

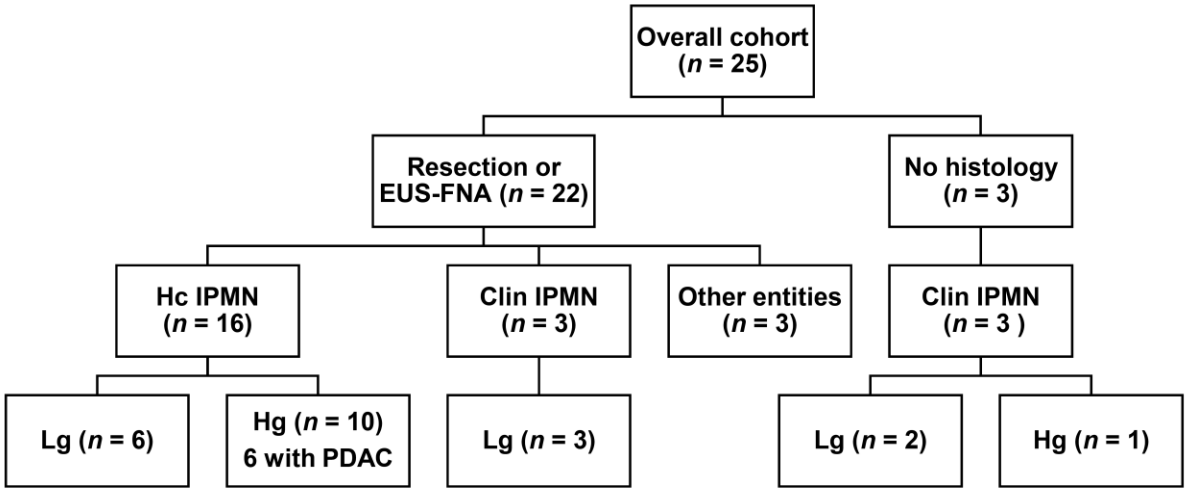

Histological diagnoses and clinical classification of 25 patients with suspected IPMN having undergone ^{68}Ga-FAPI-PET/CT. Abbreviations: EUS-FNA = endoscopic ultrasound guided fine needle aspiration, hc IPMN = histologically confirmed IPMN, clin IPMN = clinical IPMN, hg = high grade, lg = low grade, PDAC= Pancreatic ductal adenocarcinoma

Figure 2

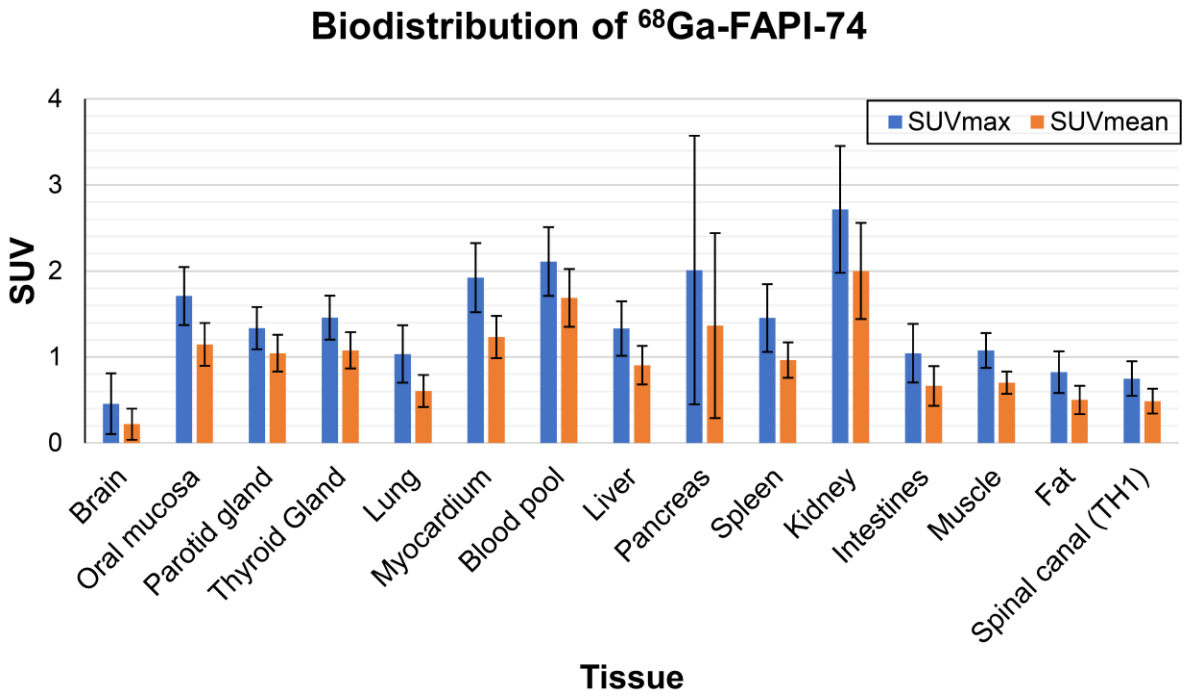

Biodistribution analysis (SUVmax and SUVmean +/- standard deviation) of 25 patients with suspected IPMN based on static PET imaging 1 h after injection of ^{68}Ga-labeled FAPI-74.

Figure 3

A

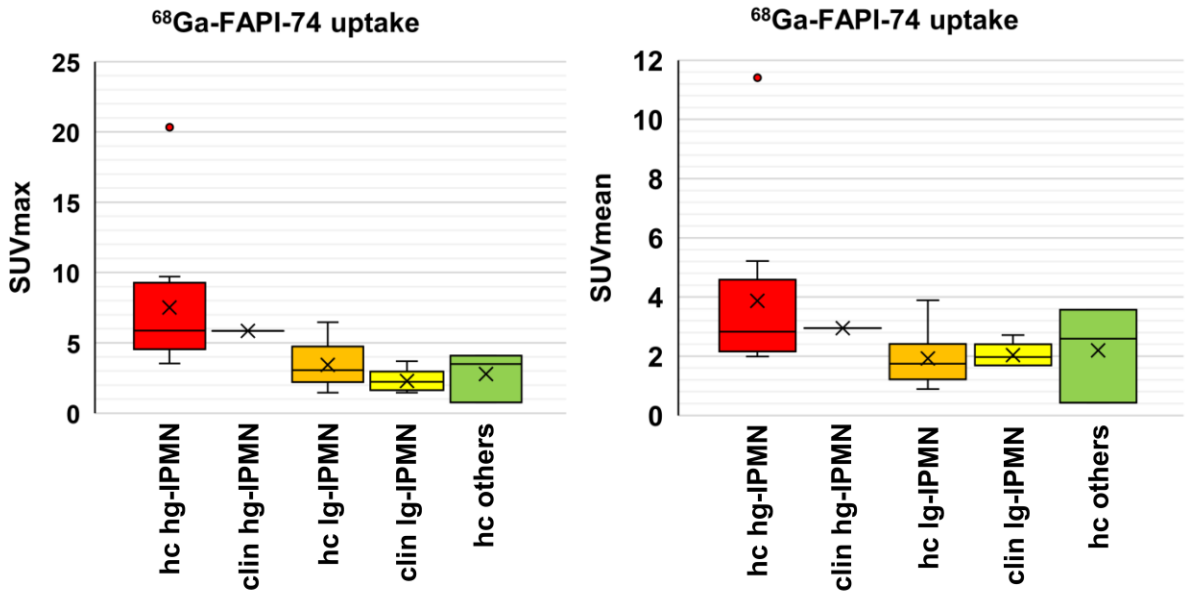

B

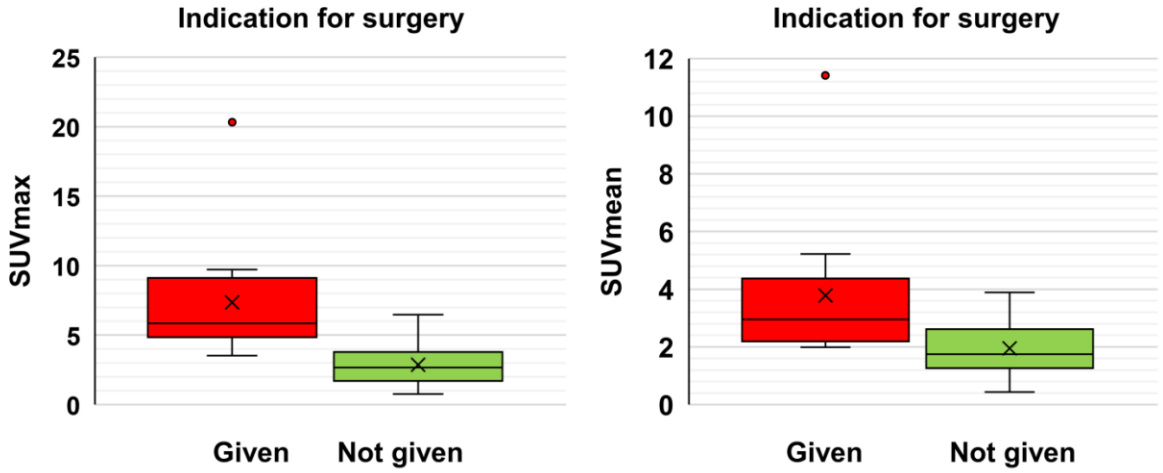

A, B Boxplots of SUVmax (A) and SUVmean (B) values of different types of cystic pancreatic lesions. Abbreviations: hc hg-IPMN = histologically confirmed high grade IPMN, clin hg-IPMN = clinical high grade IPMN, hc lg-IPMN = histologically confirmed low grade IPMN, clin lg-IPMN = clinical low grade IPMN, hc others = histologically confirmed

other entities. **C, D** Boxplots of SUVmax (C) and SUVmean (D) values sorted by given or not given indication for surgery. Boxes represent the interquartile range, whiskers the range of 1.5 IQR, horizontal line within the box indicates the median and cross the mean. Data outliers are shown separately within graph.

Figure 4

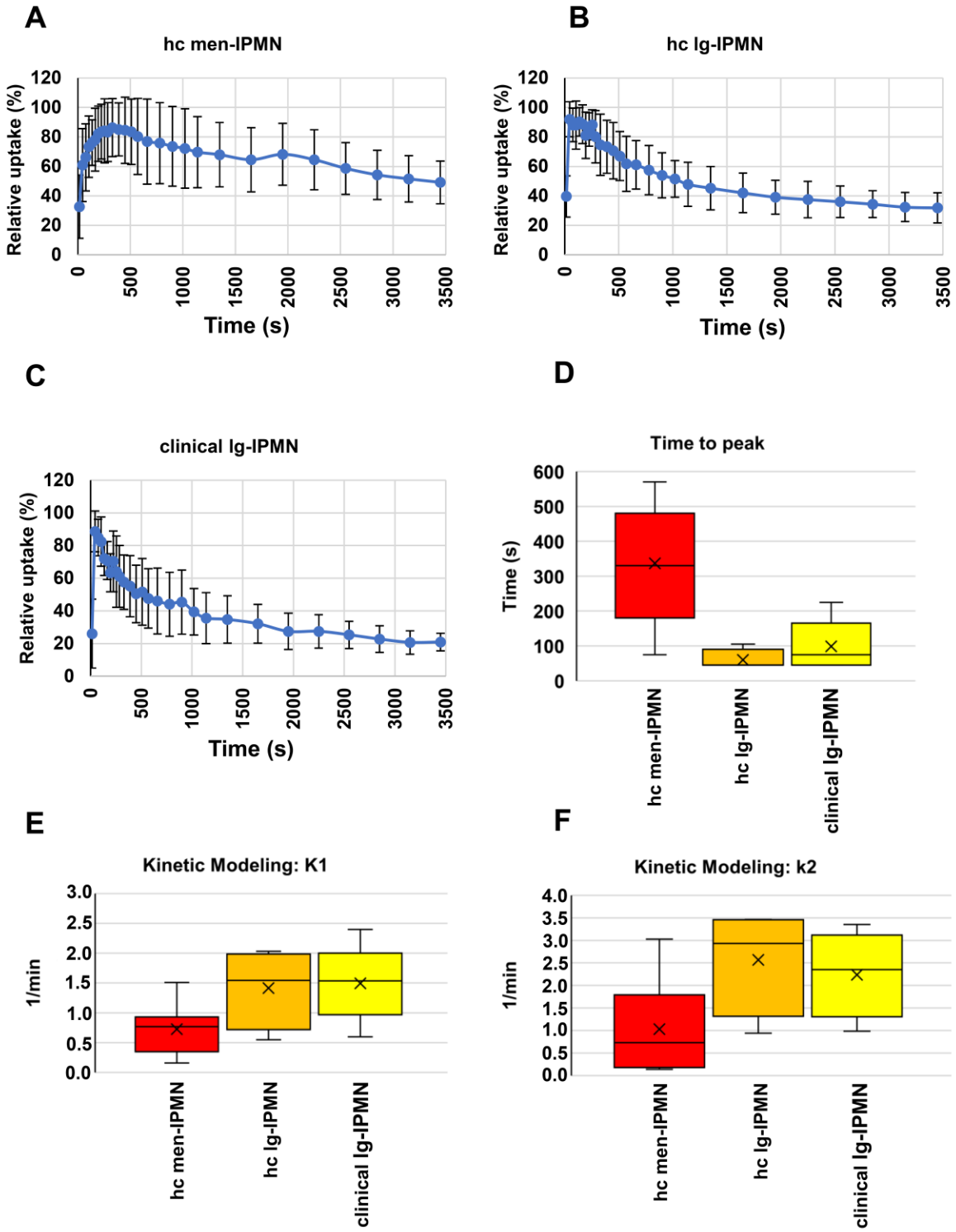
A
hc men-IPMN
Relative uptake (%)
Time (s)
B
hc lg-IPMN
Relative uptake (%)
Time (s)
C
clinical lg-IPMN
Relative uptake (%)
Time (s)
D
Time to peak
Time (s)
hc men-IPMN
hc lg-IPMN
clinical lg-IPMN
E
Kinetic Modeling: K1
1/min
hc men-IPMN
hc lg-IPMN
clinical lg-IPMN
F
Kinetic Modeling: k2
1/min
hc men-IPMN
hc lg-IPMN
clinical lg-IPMN

A, B, C Time activity curves displaying the averaged ^{68}Ga-FAPI-74 uptake (relative to the peak) kinetics of histologically confirmed menacing IPMN (hc men-IPMN) (A), histologically confirmed low grade IPMN (hc lg-IPMN) (B) and clinical low grade IPMN (clin lg-IPMN) (C). **D** Box plot displaying time to peak values of histologically confirmed menacing IPMN, histologically confirmed low grade IPMN and clinical low grade IPMN as measured by dynamic ^{68}Ga-FAPI-74 PET imaging. **E, F** Box plots displaying K1 (E) and k2 (F) values of histologically confirmed menacing IPMN, histologically confirmed low grade IPMN and clinical low grade IPMN as calculated by kinetic modeling of dynamic ^{68}Ga-FAPI-74 PET imaging data. Boxes represent the interquartile range, whiskers the range of 1.5 IQR, horizontal line within the box indicates the median and cross the mean. Data outliers are shown separately within graph.

Figure 5

A

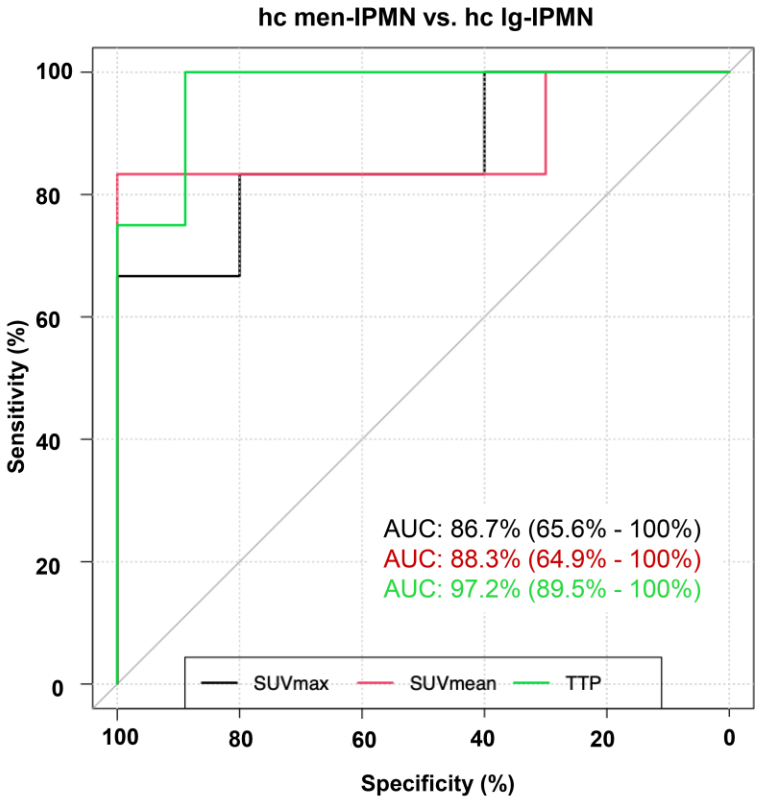
hc men-IPMN vs. hc lg-IPMN
Sensitivity (%)
Specificity (%)
100
80
60
40
20
0
AUC: 86.7% (65.6% - 100%)
AUC: 88.3% (64.9% - 100%)
AUC: 97.2% (89.5% - 100%)
SUVmax
SUVmean
TTP

B

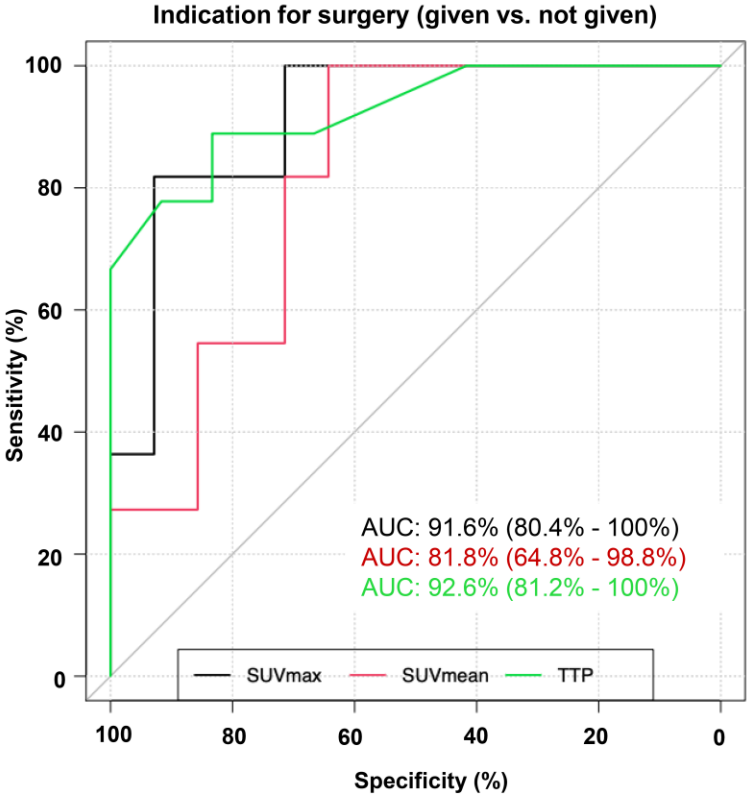
Indication for surgery (given vs. not given)
Sensitivity (%)
Specificity (%)
100
80
60
40
20
0
AUC: 91.6% (80.4% - 100%)
AUC: 81.8% (64.8% - 98.8%)
AUC: 92.6% (81.2% - 100%)
SUVmax
SUVmean
TTP

A, B Receiver operating characteristic (ROC) curves depicting the sensitivity and specificity of quantitative static (SUVmax and SUVmean) and dynamic (TTP) ^{68}Ga-FAPI-74 PET parameters for the differentiation of histologically confirmed menacing IPMN and low grade IPMN (A) and of lesions with and without indication for surgery (B). Abbreviation: AUC = area under the curve.

Figure 6

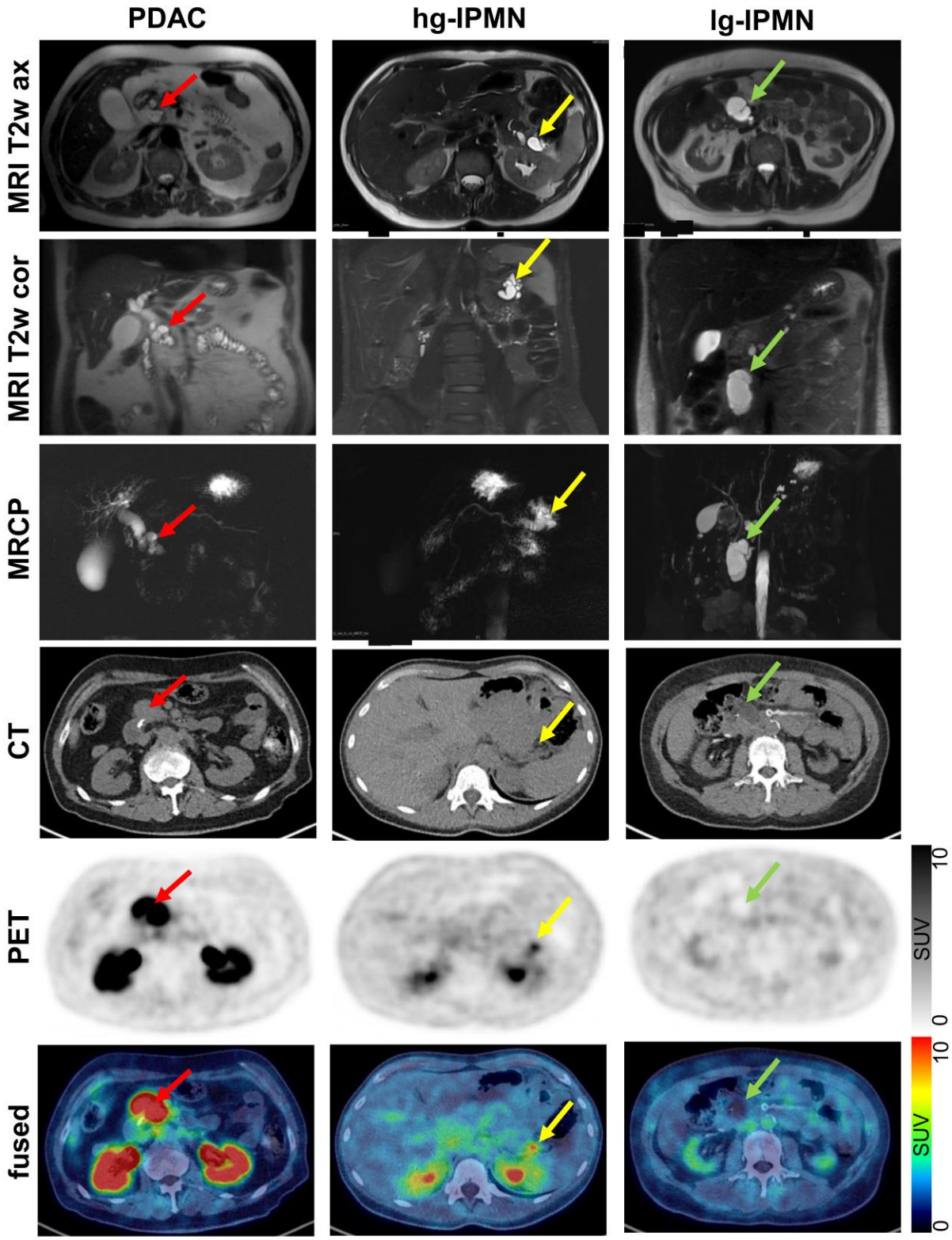
PDAC
hg-IPMN
lg-IPMN
MRI T2w ax
MRI T2w cor
MRCP
CT
PET
fused
SUV
10
0
SUV
10
0

Representative axial and coronal T2 weighted magnetic resonance imaging (MRI T2w ax, MRI T2w cor), magnetic resonance cholangiopancreatography (MRCP), axial computed tomography (CT ax), axial positron emission tomography (PET ax) and fused images of a patient with hc hg-IPMN with progression into PDAC, a patient with hg-IPMN without PDAC and Patient with lg-IPMN. Red, yellow and green arrows indicate the pathologies.

References

1. Park W, Chawla A, O'Reilly EM. Pancreatic Cancer: A Review. *JAMA.* 2021;326:851-862.

2. Rezaee N, Barbon C, Zaki A, et al. Intraductal papillary mucinous neoplasm (IPMN) with high-grade dysplasia is a risk factor for the subsequent development of pancreatic ductal adenocarcinoma. *HPB (Oxford).* 2016;18:236-246.

3. Tanaka M, Fernandez-Del Castillo C, Kamisawa T, et al. Revisions of international consensus Fukuoka guidelines for the management of IPMN of the pancreas. *Pancreatology.* 2017;17:738-753.

4. European Study Group on Cystic Tumours of the P. European evidence-based guidelines on pancreatic cystic neoplasms. *Gut.* 2018;67:789-804.

5. Fritz S, Buchler MW, Werner J. [Surgical therapy of intraductal papillary mucinous neoplasms of the pancreas]. *Chirurg.* 2012;83:130-135.

6. Schnelldorfer T, Sarr MG, Nagorney DM, et al. Experience with 208 resections for intraductal papillary mucinous neoplasm of the pancreas. *Arch Surg.* 2008;143:639-646; discussion 646.

7. de Jong K, van Hooft JE, Nio CY, et al. Accuracy of preoperative workup in a prospective series of surgically resected cystic pancreatic lesions. *Scand J Gastroenterol.* 2012;47:1056-1063.

8. Morris-Stiff G, Lentz G, Chalikonda S, et al. Pancreatic cyst aspiration analysis for cystic neoplasms: mucin or carcinoembryonic antigen--which is better? *Surgery.* 2010;148:638-644; discussion 644-635.

9. Heckler M, Brieger L, Heger U, et al. Predictive performance of factors associated with malignancy in intraductal papillary mucinous neoplasia of the pancreas. *BJS Open.* 2018;2:13-24.

10. Tjaden C, Sandini M, Mihaljevic AL, et al. Risk of the Watch-and-Wait Concept in Surgical Treatment of Intraductal Papillary Mucinous Neoplasm. *JAMA Surg.* 2021;156:818-825.

11. von Ahrens D, Bhagat TD, Nagrath D, Maitra A, Verma A. The role of stromal cancer-associated fibroblasts in pancreatic cancer. *J Hematol Oncol.* 2017;10:76.

12. Hanahan D, Weinberg RA. Hallmarks of cancer: the next generation. *Cell.* 2011;144:646-674.

13. Lindner T, Loktev A, Altmann A, et al. Development of Quinoline-Based Theranostic Ligands for the Targeting of Fibroblast Activation Protein. *J Nucl Med.* 2018;59:1415-1422.

14. Lindner T, Altmann A, Giesel F, et al. (18)F-labeled tracers targeting fibroblast activation protein. *EJNMMI Radiopharm Chem.* 2021;6:26.

15. Loktev A, Lindner T, Mier W, et al. A Tumor-Imaging Method Targeting Cancer-Associated Fibroblasts. *J Nucl Med.* 2018;59:1423-1429.

16. Rohrich M, Leitz D, Glatting FM, et al. Fibroblast Activation Protein-Specific PET/CT Imaging in Fibrotic Interstitial Lung Diseases and Lung Cancer: A Translational Exploratory Study. *J Nucl Med.* 2022;63:127-133.

17. DeLong ER, DeLong DM, Clarke-Pearson DL. Comparing the areas under two or more correlated receiver operating characteristic curves: a nonparametric approach. *Biometrics.* 1988;44:837-845.

18. Robin X, Turck N, Hainard A, et al. pROC: an open-source package for R and S+ to analyze and compare ROC curves. *BMC Bioinformatics.* 2011;12:77.

19. Rohrich M, Naumann P, Giesel FL, et al. Impact of (68)Ga-FAPI-PET/CT imaging on the therapeutic management of primary and recurrent pancreatic ductal adenocarcinomas. *J Nucl Med.* 2020.

20. Kratochwil C, Flechsig P, Lindner T, et al. (68)Ga-FAPI PET/CT: Tracer Uptake in 28 Different Kinds of Cancer. *J Nucl Med.* 2019;60:801-805.

21. Wang S, Zhou X, Xu X, et al. Dynamic PET/CT Imaging of (68)Ga-FAPI-04 in Chinese Subjects. *Front Oncol.* 2021;11:651005.

22. Geist BK, Xing H, Wang J, et al. A methodological investigation of healthy tissue, hepatocellular carcinoma, and other lesions with dynamic (68)Ga-FAPI-04 PET/CT imaging. *EJNMMI Phys.* 2021;8:8.

23. Fritz S, Klauss M, Bergmann F, et al. Pancreatic main-duct involvement in branch-duct IPMNs: an underestimated risk. *Ann Surg.* 2014;260:848-855; discussion 855-846.

24. Roch AM, Ceppa EP, DeWitt JM, et al. International Consensus Guidelines parameters for the prediction of malignancy in intraductal papillary mucinous neoplasm are not properly weighted and are not cumulative. *HPB (Oxford).* 2014;16:929-935.

25. Goh BK, Thng CH, Tan DM, et al. Evaluation of the Sendai and 2012 International Consensus Guidelines based on cross-sectional imaging findings performed for the initial triage of mucinous cystic lesions of the pancreas: a single institution experience with 114 surgically treated patients. *Am J Surg.* 2014;208:202-209.

26. Sahora K, Mino-Kenudson M, Brugge W, et al. Branch duct intraductal papillary mucinous neoplasms: does cyst size change the tip of the scale? A critical analysis of the revised international consensus guidelines in a large single-institutional series. *Ann Surg.* 2013;258:466-475.

27. Aso T, Ohtsuka T, Matsunaga T, et al. "High-risk stigmata" of the 2012 international consensus guidelines correlate with the malignant grade of branch duct intraductal papillary mucinous neoplasms of the pancreas. *Pancreas.* 2014;43:1239-1243.

28. Nguyen AH, Toste PA, Farrell JJ, et al. Current recommendations for surveillance and surgery of intraductal papillary mucinous neoplasms may overlook some patients with cancer. *J Gastrointest Surg.* 2015;19:258-265.

29. Dortch JD, Stauffer JA, Asbun HJ. Pancreatic Resection for Side-Branch Intraductal Papillary Mucinous Neoplasm (SB-IPMN): a Contemporary Single-Institution Experience. *J Gastrointest Surg.* 2015;19:1603-1609.

30. Robles EP, Maire F, Cros J, et al. Accuracy of 2012 International Consensus Guidelines for the prediction of malignancy of branch-duct intraductal papillary mucinous neoplasms of the pancreas. *United European Gastroenterol J.* 2016;4:580-586.

31. Seo N, Byun JH, Kim JH, et al. Validation of the 2012 International Consensus Guidelines Using Computed Tomography and Magnetic Resonance Imaging: Branch Duct and Main Duct Intraductal Papillary Mucinous Neoplasms of the Pancreas. *Ann Surg.* 2016;263:557-564.

32. Hackert T, Fritz S, Klauss M, et al. Main-duct Intraductal Papillary Mucinous Neoplasm: High Cancer Risk in Duct Diameter of 5 to 9 mm. *Ann Surg.* 2015;262:875-880; discussion 880-871.

33. Abdeljawad K, Vemulapalli KC, Schmidt CM, et al. Prevalence of malignancy in patients with pure main duct intraductal papillary mucinous neoplasms. *Gastrointest Endosc.* 2014;79:623-629.

34. Kawada N, Uehara H, Nagata S, Tsuchishima M, Tsutsumi M, Tomita Y. Mural nodule of 10 mm or larger as predictor of malignancy for intraductal papillary mucinous neoplasm of the pancreas: Pathological and radiological evaluations. *Pancreatology.* 2016;16:441-448.

35. Kobayashi N, Sugimori K, Shimamura T, et al. Endoscopic ultrasonographic findings predict the risk of carcinoma in branch duct intraductal papillary mucinous neoplasms of the pancreas. *Pancreatology.* 2012;12:141-145.

36. Shimizu Y, Yamaue H, Maguchi H, et al. Predictors of malignancy in intraductal papillary mucinous neoplasm of the pancreas: analysis of 310 pancreatic resection patients at multiple high-volume centers. *Pancreas.* 2013;42:883-888.

37. Best LM, Rawji V, Pereira SP, Davidson BR, Gurusamy KS. Imaging modalities for characterising focal pancreatic lesions. *Cochrane Database Syst Rev.* 2017;4:CD010213.

38. Xu MM, Yin S, Siddiqui AA, et al. Comparison of the diagnostic accuracy of three current guidelines for the evaluation of asymptomatic pancreatic cystic neoplasms. *Medicine (Baltimore).* 2017;96:e7900.

39. Sultana A, Jackson R, Tim G, et al. What Is the Best Way to Identify Malignant Transformation Within Pancreatic IPMN: A Systematic Review and Meta-Analyses. *Clin Transl Gastroenterol.* 2015;6:e130.

40. Bertagna F, Treglia G, Baiocchi GL, Giubbini R. F18-FDG-PET/CT for evaluation of intraductal papillary mucinous neoplasms (IPMN): a review of the literature. *Jpn J Radiol.* 2013;31:229-236.

41. Regenet N, Sauvanet A, Muscari F, et al. The value of (18)F-FDG positron emission tomography to differentiate benign from malignant intraductal papillary mucinous neoplasms: A prospective multicenter study. *J Visc Surg.* 2020;157:387-394.

42. Liu H, Cui Y, Shao J, Shao Z, Su F, Li Y. The diagnostic role of CT, MRI/MRCP, PET/CT, EUS and DWI in the differentiation of benign and malignant IPMN: A meta-analysis. *Clin Imaging.* 2021;72:183-193.

Graphical Abstract

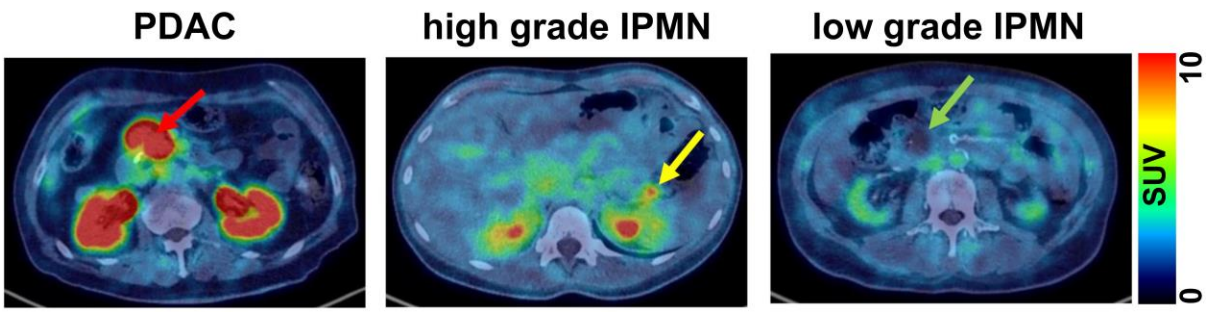

Supplemental figure 1

A

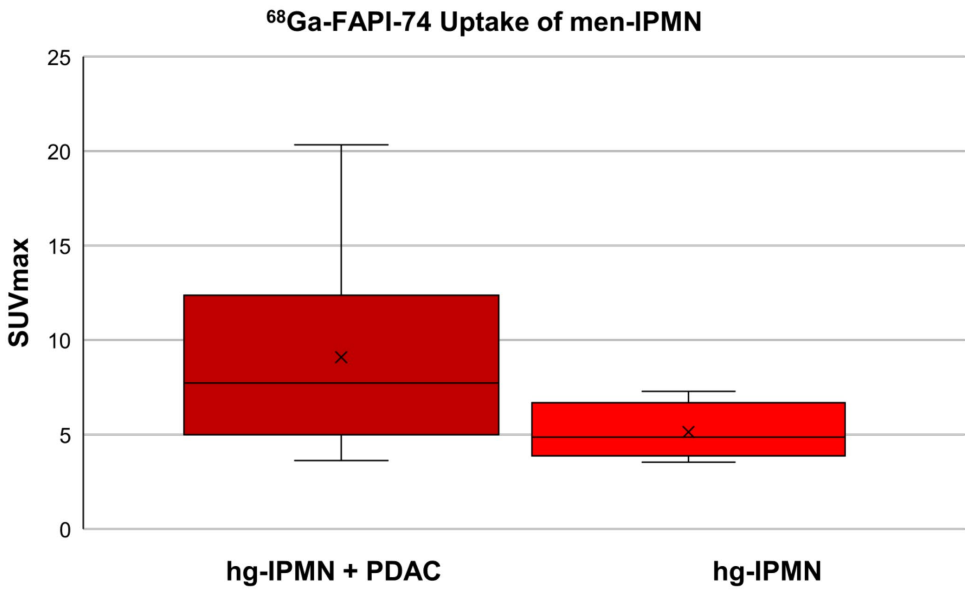

B

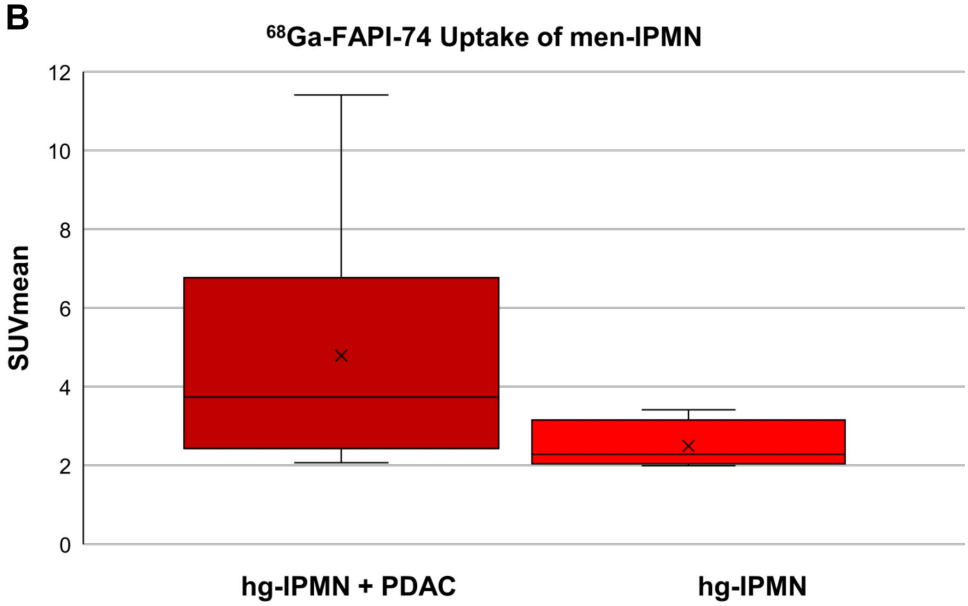

A,B Boxplots of SUVmax (A) and SUVmean (B) values of high grade IPMN with and without PDAC. Boxes represent the interquartile range, whiskers the range of 1.5 IQR, horizontal line within the box indicates the median and cross the mean. Data outliers are shown separately within graph.

Supplemental figure 2

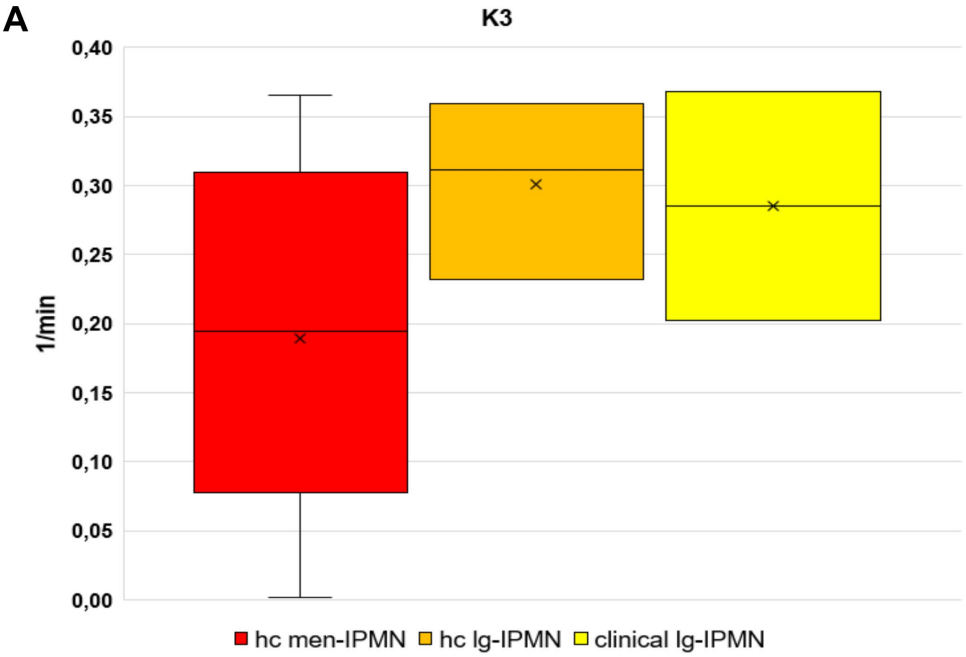

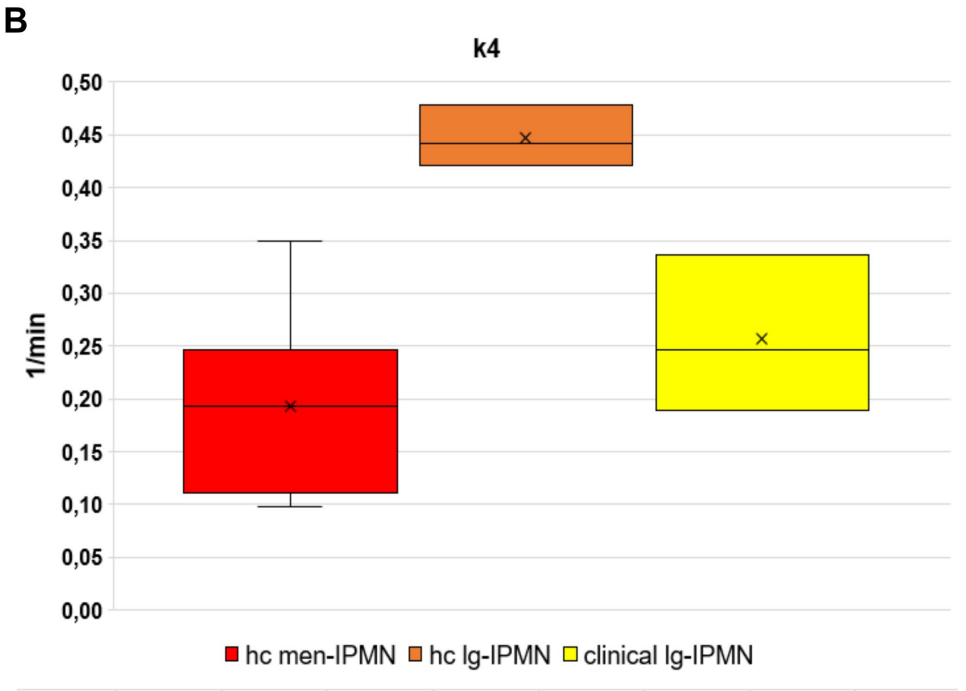

A,B Box plots displaying K3 (A) and k4 (B) values of histologically confirmed menacing IPMN, histologically confirmed low grade IPMN and clinically low grade IPMN as calculated by kinetic modeling of dynamic ^{68}Ga-FAPI-74 PET imaging data. Boxes represent the interquartile range, whiskers the range of 1.5 IQR, horizontal line within the box indicates the median and cross the mean. Data outliers are shown separately within graph.